Article

Quantitative Single Molecule Measurements on the Interaction Forces of Poly(l-glutamic acid) with Calcite Crystals

Lars Sonnenberg, Yufei Luo, Helmut Schlaad, Markus Seitz, Helmut Clfen, and Hermann E. Gaub

J. Am. Chem. Soc., **2007**, 129 (49), 15364-15371 • DOI: 10.1021/ja074070i

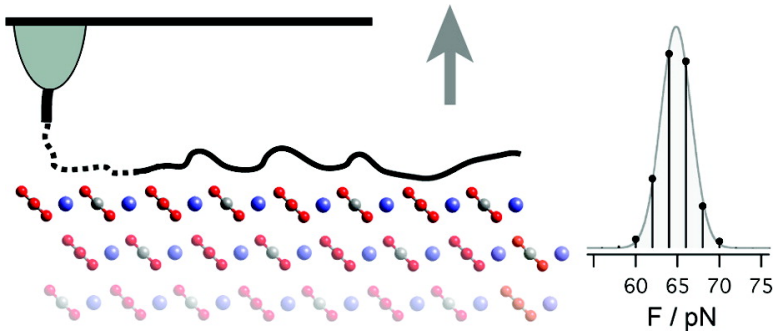

More About This Article

Additional resources and features associated with this article are available within the HTML version:

- Supporting Information
- Access to high resolution figures
- Links to articles and content related to this article
- Copyright permission to reproduce figures and/or text from this article

View the Full Text HTML

J|A|C|S
ARTICLES
Published on Web 11/16/2007

Quantitative Single Molecule Measurements on the Interaction Forces of Poly(L-glutamic acid) with Calcite Crystals

Lars Sonnenberg,*,† Yufei Luo,‡ Helmut Schlaad,‡ Markus Seitz,†
Helmut Cölfen,*,‡ and Hermann E. Gaub†

Contribution from the Lehrstuhl für Angewandte Physik and Center for NanoScience, Ludwig-Maximilians-Universität München, Amalienstrasse 54, 80799 München, Germany, and Max-Planck-Institute of Colloids and Interfaces, Colloid Chemistry, Research Campus Golm, 14424 Potsdam, Germany

Received June 5, 2007; E-mail: sonnenberg@physik.uni-muenchen.de; coelfen@mpikg.mpg.de

Abstract: The interaction between poly(L-glutamic acid) (PLE) and calcite crystals was studied with AFM-based single molecule force spectroscopy. Block copolymers of poly(ethylene oxide) (PEO) and PLE were synthesized and covalently attached to the tip of an AFM cantilever. In desorption measurements the molecules were allowed to adsorb on the calcite crystal faces and afterward successively desorbed. The corresponding desorption forces were detected with high precision, showing for example a force transition between the two blocks. Because of its importance in the crystallization process in biominerals, the PLE-calcite interaction was investigated as a function of the pH as well as the calcium concentration of the aqueous solution. The sensitivity of the technique was underlined by resolving different interaction forces for calcite (104) and calcite (100).

Introduction

Biominerals are composite or hybrid materials consisting of an inorganic crystal phase and an organic phase with outstanding materials properties and hierarchical organization.[1] These advanced features are the result of a precise control of crystallization and self-organization processes by soluble and insoluble organic molecules. Biominerals are thus considered as archetypes for future advanced materials.

Many of the soluble organic polymers, which can be extracted from biominerals, are extraordinarily acidic.[2−5] Matrix proteins in biominerals typically contain 30−40% of aspartic acid (D) or glutamic acid (E) residues.[6,7] The acidic residues can interact with calcium, which is the basis for many biominerals like calcium carbonates and phosphates. Acidic macromolecules are therefore considered to play a key role in biomineralization processes.[5] On the basis of this knowledge, synthetic model polymers have been designed and widely applied for the control of crystallization processes.[8,9] Especially successful are the so-called double hydrophilic block copolymers, which allow for a precise control of crystallization because of the separation of binding and stabilizing moieties.[10,11] Nevertheless, detailed and quantitative knowledge of the polymer−crystal interaction is still lacking and with it a quantitative explanation for face-specific polymer binding (e.g., certain acidic proteins interact selectively in vitro with calcite crystal faces[12,13]), which could verify computer modeling predictions on such interactions.[14] It is therefore not only important for the fundamental understanding of biomineralization processes to quantify the polymer−crystal interactions but also for the understanding of additive-controlled crystallization in general concerning topics such as face-selective polymer adsorption,[9,12,13] oriented attachment,[15] or mesocrystal formation,[16] where face-selective additive adsorption is of importance for the subsequent morphogenesis process by self-assembly to ordered nanoparticle superstructures or by further crystal growth. The collection of such data is thus a most important prerequisite to transfer the lessons from nature into the synthetic materials world.

AFM-based single-molecule force spectroscopy allows for the precise measurement of the interaction forces of single polymers with solid (mineral) surfaces.[17,18] In so-called desorp-

† Ludwig-Maximilians-Universität München.
‡ Max-Planck-Institute of Colloids and Interfaces.

(1) Mann, S. *Biomineralization: Principles and Concepts in Bioinorganic Materials Chemistry*; Oxford University Press: New York, 2001.
(2) Lowenstam, H. A.; Weiner, S. *On Biomineralization*; Oxford University Press: New York, 1989.
(3) Simkiss, K.; Wilbur, K. M. *Biomineralization: cell biology and mineral deposition*; Academic Press: San Diego, 1989.
(4) Wheeler, A. P.; Sikes, C. S.; Williams, R. J. P., Ed.; VCH: Weinheim, 1989; p 95.
(5) Gotliv, B. A.; Kessler, N.; Sumerel, J. L.; Morse, D. E.; Tuross, N.; Addadi, L.; Weiner, S. *ChemBioChem* **2005**, *6*, 304−314.
(6) Weiner, S. *Calcif. Tissue Int.* **1979**, *29*, 163−167.
(7) Wheeler, A. P.; Low, K. C.; Sikes, C. S. ACS Symposium Series 444; American Chemical Society: Washington, DC, 1991; pp 72−84.
(8) Xu, A. W.; Ma, Y. R.; Cölfen, H. *J. Mater. Chem.* **2007**, *17*, 415−449.
(9) Cölfen, H. *Top. Curr. Chem.* **2007**, *271*, 1−77.
(10) Cölfen, H. *Macromol. Rapid Commun.* **2001**, *22*, 219−252.
(11) Yu, S. H.; Cölfen, H. *J. Mater. Chem.* **2004**, *14*, 2124−2147.
(12) Addadi, L.; Berkovitchyellin, Z.; Weissbuch, I.; Vanmil, J.; Shimon, L. J. W.; Lahav, M.; Leiserowitz, L. *Angew. Chem., Int. Ed.* **1985**, *24*, 466−485.
(13) Addadi, L.; Weiner, S. *Angew. Chem., Int. Ed.* **1992**, *31*, 153−169.
(14) Shi, W. Y.; Wang, F. Y.; Xia, M. Z.; Lei, W.; Zhang, S. G. *Acta Chim. Sinica* **2006**, *64*, 1817−1823.
(15) Wang, T. X.; Reinecke, A.; Cölfen, H. *Langmuir* **2006**, *22*, 8986−8994.
(16) Cölfen, H.; Antonietti, M. *Angew. Chem., Int. Ed.* **2005**, *44*, 5576−5591.
(17) Seitz, M.; Friedsam, C.; Jöstl, W.; Hugel, T.; Gaub, H. E. *ChemPhysChem* **2003**, *4*, 986−990.

10.1021/ja074070i CCC: $37.00

tion measurements single molecules are covalently attached to an AFM tip and are allowed to adsorb on the mineral substrate. Then, they are successively desorbed in an equilibrium process by separating the AFM tip from the substrate surface (Figure 3). The measured force−distance traces exhibit plateaus of constant force, from which the specific interaction of the polymeric molecules and the mineral surface can be obtained in a quantitative manner.

In order to elucidate the yet unknown polymer interaction with the mineral phase, we have applied AFM-desorption measurements to quantitatively investigate the interaction of poly(L-glutamic acid) (PLE) with calcite ($CaCO_3$) crystal faces on the single molecule level. For this, a triblock copolymer consisting of a polyamine block for chemical coupling to the AFM tip, a PEO block as hydrophilic spacer, and the PLE block as interacting block was synthesized and coupled to the AFM tip. In the context of this study, two key aspects were addressed: (a) The impact of experimental conditions (pH, Ca-concentration) on the molecular interaction of PLE with the calcite surface, and (b) the impact of crystal face on the molecular interaction of PLE with the calcite surface.

Materials and Methods

Polymer Synthesis (Polyamine-*b*-PEO-*b*-PLE). A double hydrophilic block copolymer consitsting of poly(ethylene oxide) (PEO) and poly(L-glutamic acid) (PLE) and which also carries primary amine functions was designed for the AFM-based single molecule force spectroscopy measurements. The polyamine block allows for the covalent attachment of the block copolymer to the AFM tip with high efficiency and long-term stability because of the multiple binding sites (see also further below). For this study the PLE was of main importance as its interaction with calcite crystal surfaces was investigated. The PEO has been included for several reasons: (i) PEO-*b*-PLE form together a double hydrophilic block copolymer, which are of special importance for drug delivery,[19] as crystallization additive or particle stabilizer in water (ref 10), (ii) in single molecule force spectroscopy experiments by means of an AFM, PEO is often used as a spacer to avoid interactions of the molecules of interest with the (tip) surface. All reagents and solvents were purchased from Sigma-Aldrich. The synthetic pathway is visualized in Figure 1.

***ω*-Hydroxy-polybutadiene-*block*-poly(ethylene oxide) (PB-*b*-PEO-OH).** PB-*b*-PEO-OH was synthesized by anionic polymerization of ethylene oxide (EO) using an *ω*-hydroxy-1,2-polybutadiene (average number of repeating units: 40), as reported by Justynska et al.[20] The characterization with nuclear magnetic resonance spectroscopy (NMR) and size exclusion chromatography (SEC) yielded the following results: ^{1}H NMR: mole fraction EO = 0.87, SEC:PDI = 1.05 (apparent polydispersity index).

***ω*-Amino-polybutadiene-*block*-poly(ethylene oxide) (PB-*b*-PEO-NH_2).** (a) PB-*b*-PEO-OH (0.5 g) was dissolved in 20 mL of CH_2Cl_2, and then *p*-tosyl chloride (0.19 g) and triethylamine (0.095 g) were added under an argon atmosphere. The solution was heated to reflux overnight. The solution was afterward concentrated to about 5 mL and precipitated into diethyl ether. The product (PB-*b*-PEO-OTos) was collected through centrifugation, reprecipitated three times, and dried in vacuum.

(b) In a 25 mL three-necked round-bottom flask, PB-*b*-PEO-OTos (0.2 g), potassium phthalimide (0.093 g) and tetra-*n*-butylammonium bromide (0.02 g) were suspended in 10 mL of *N*,*N*-dimethylformamide (DMF) under vigorous stirring. The mixture was gradually warmed to 100 °C in an oil bath and stirred at this temperature overnight. After cooling down to room temperature, the mixture was condensed to 2 mL and precipitated into diethyl ether. The obtained yellow solid was dissolved in $CHCl_3$ and the solution passed through a filter. The product (PB-*b*-PEO-phthalimide) was then precipitated again in diethyl ether and dried in vacuum.

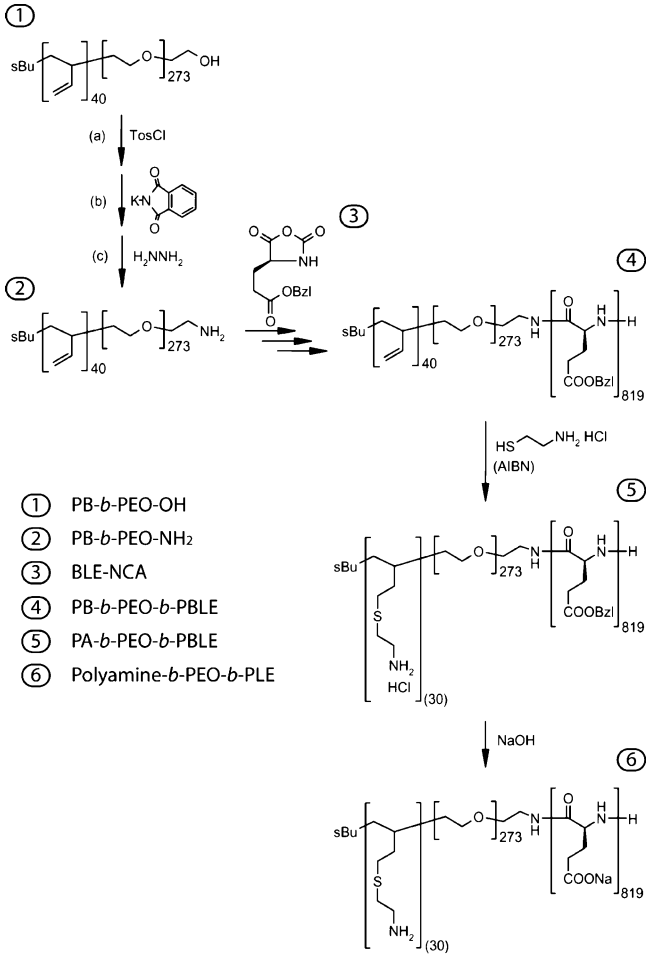

Figure 1. Schematics of the synthesis of PEO-*b*-PLE carrying primary amine functions.

(c) PB-*b*-PEO-phthalimide (0.2 g) was dissolved in a mixture of dioxane (20 mL) and methanol (10 mL), and then hydrazine monohydrate (1 mL) was added. The solution was heated to reflux with stirring overnight. After the solvent was evaporated, 0.5 N aqueous HCl was added and the mixture stirred for 15 min. After dilution with 15 mL of water and heating for 1 h, the solution was filtered and dialyzed against deionized water (MWCO: 3500 Da). The PB-*b*-PEO-NH_2 was then isolated by freeze-drying.

***γ*-Benzyl L-Glutamate-*N*-carboxyanhydride (BLE-NCA).** *γ*-Benzyl L-glutamate (5 g) was suspended in a mixture of α-pinene (6.57 mL, 5.74 g) and ethyl acetate (20 mL) (freshly distilled from CaH_2). The suspension was heated to reflux (76 °C), and a solution of triphosgene (3.13 g) in ethyl acetate (9.5 mL) was slowly added under stirring. After a clear solution was formed, 75 mL of heptane was slowly added under good stirring. The solution was cooled to −10 °C, kept overnight at this temperature, and then rapidly filtered. The solid NCA was recrystallized twice from ethyl acetate/heptane 1:4 (v/v), washed twice with heptane, and dried in vacuum at room temperature.[21]

Polybutadiene-*block*-poly(ethylene oxide)-*block*-poly(*γ*-benzyl L-glutamate) (PB-*b*-PEO-*b*-PBLE). PB-*b*-PEO-NH_2 and BLE-NCA

(18) Smith, B. L.; Schaffer, T. E.; Viani, M.; Thompson, J. B.; Frederick, N. A.; Kindt, J.; Belcher, A.; Stucky, G. D.; Morse, D. E.; Hansma, P. K. *Nature* **1999**, *399*, 761−763.
(19) Kataoka, K.; Harada, A.; Nagasaki, Y. *Adv. Drug Delivery Rev.* **2001**, *47*, 113−131.
(20) Justynska, J.; Hordyjewicz, Z.; Schlaad, H. *Polymer* **2005**, *46*, 12057−12064.
(21) ISOCHEM. French Patent EP 1 201 659 A1, 2002.

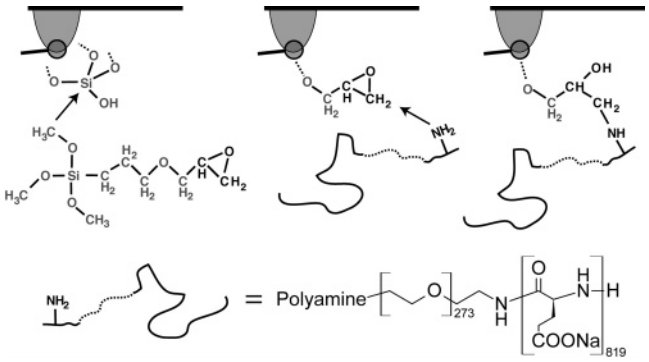

Figure 2. Attachment of PEO-*b*-PLE carrying primary amine functions at the α-chain end to an epoxy-functionalized AFM tip.

were weighted in separate two-neck flasks and dried overnight at room temperature in vacuum. The flasks were filled with argon and DMF (distilled from CaH_2 and from P_2O_5) was added (3 mL and 5 mL, respectively). The mixtures were stirred at room temperature until complete dissolution, and then the solution of the NCA was added to the polymer via a transfer needle. The combined solution was stirred for 3 days at 60 °C, and then the solution was cooled down to room temperature and concentrated to 3 mL. The product was afterward precipitated into diethyl ether and dried under reduced pressure.

^{1}H NMR: 819 BLE repeating units, SEC: PDI = 1.4 (apparent polydispersity index) (see Supporting Information, Figures SI-1 and SI-2).

Poly(4-(2-(amino hydrochloride)-ethylthio)-butylene)-*block*-poly-(ethylene oxide)-*block*-poly(γ-benzyl L-glutamate) (PA-*b*-PEO-*b*-PBLE). In a 25 mL three-necked round-bottom flask, PB-*b*-PEO-*b*-PBLE (0.150 g) and 2-aminoethanethiol hydrochloride (0.023 g) were dissolved in 5 mL of DMF. Under stirring, the solution was saturated with nitrogen for 30 min. Azoisobutyronitrile (AIBN, 0.004 g) was then added, and the solution was stirred for 24 h at 60 °C. The product was precipitated into diethyl ether, filtered, redissolved in DMF/water 1:1 (v/v), and dialyzed against deionized water. After freeze-drying, the triblock copolymer with pendant amine groups was obtained as a white powder.

About 30 amino groups should be attached to the α-chain end of PEO-*b*-PBLE, considering an efficiency of thiol addition of ∼75% (see ref 20).

Poly(4-(2-amino-ethylthio)-butylene)-*block*-poly(ethylene oxide)-*block*-poly(L-glutamate) (Polyamine-*b*-PEO-*b*-PLE). The polyamine-*b*-PEO-*b*-PBLE (0.100 g) was dissolved in a mixture of DMF (5 mL) and water (5 mL), and the solution was saturated with nitrogen for 10 min. A 0.1 N NaOH (0.5 mL) solution was added under stirring, and the solution was stirred overnight at room temperature. The solution was then dialyzed and freeze-dried to obtain the triblock copolymer polyamine-*b*-PEO-*b*-PLE.

Modification of AFM Tips. Epoxy-functionalized AFM tips for the covalent attachment of polyamines were obtained by treating the Si_3N_4 tip (Microlever, Veeco Instruments) with (3-glycidyloxypropyl)trimethoxysilane for 30 s and rinsing with toluene and water three times. Afterward the polymers were immediately attached to the AFM tip by soaking it in an aqueous solution of polyamine-*b*-PEO-*b*-PLE (concentration 0.25 mg/mL) for 90 min (Figure 2). After rinsing with water, the modified tip was dried with nitrogen.

AFM Desorption Experiments. In desorption experiments[17,22−25] single polymer chains covalently attached to the AFM tip are adsorbed on a solid surface and afterward successively desorbed by separating tip and surface. When the tip is approaching the bare surface, polymers will adsorb onto it. When retracting the AFM tip, the molecules successively desorb from the surface. Therefore, desorption takes place under equilibrium conditions because of the much faster dynamics of the polymer-surface contacts in comparison to the retraction velocity of the AFM tip (ca. 1 μm/s). In other words, the polymers are highly mobile on the surface and are able to rearrange on the surface rather than being pinned to the surface.[26] As a consequence, the polymer chains are simply "pulled-off" the surface and the desorption process is not loading-rate-dependent, i.e., the detected force is not a function of the retraction velocity of the cantilever. Under these conditions the desorption process manifests itself as a plateau of constant force in the force−distance curves. The height of the force plateau represents the magnitude of the desorption force between the polymer chain and the surface, and the mean desorption force is obtained by a statistical analysis. Note that the desorption force can only be determined with high accuracy from the last plateau (F_{des} in Figure 3), as no intermolecular interactions are contributing here.

In the case of low lateral mobility of the polymers, the observed force−extension traces are significantly altered; the flat desorption plateaus pass into stretching curves (from which the elasticity of single polymer chains can be deduced) or a combination of both.[26,27] However, if the lateral mobility of the polymers is high as throughout in the experiments described here, the molecules rearrange on the surface to maximize the adsorption enthalpy. Flat force plateaus in the force−extension spectra are then obtained even on rough surfaces (e.g., etched silicon nitride).[28,29] That is, the surface roughness or surface structures (e.g., steps on the calcite surface) are not reflected in the measurements curves under these conditions.

Moreover, the distance at which the plateau force drops to zero (plateau length) denotes the complete detachment of the polymer from the surface, and thus the number of observed plateaus equals the number of desorbed polymer chains.

The AFM desorption measurements were conducted with a home-built instrument. Nominal spring constants of the cantilevers were calibrated using the thermal oscillation method. Because of the calculated spring constants may have deviations of up to 10%, a single tip was used for an entire set of measurement series to monitor minute force differences. Thereby, every measurement series consists of 750−1000 force−distance curves. As a consequence, the binding of the polymers to the tip had to be very robust because for every tip about 20000 force−distance curves had to be recorded. The usage of a polyamine-block for attaching the molecules to the tip proved to be highly efficient and have long-term stability because of the multiple binding sites.

The covalent attachment of the block copolymer PEO_{273}-*b*-PLE_{819} to the AFM tip allows for studying the interaction of both the PEO and the PLE with the calcite surface in a single experiment. Figure 4 shows a force plateau as obtained by continuously desorbing the block copolymer from the calcite (104) face in an aqueous solution of 10 mM $CaCl_2$. It may be important to point out that because of the attachment of the polymer to the AFM tip via the amine functions, the PEO block is first desorbed and then the PLE block (see Figures 2 and 3). This means that at distances larger than the contour length of the PEO_{273} (∼100 nm), the measured desorption force exclusively originates from the desorption of PLE monomers.

The interaction force of the PLE is slightly higher than that of PEO, as qualitatively expected, because PEO is not supposed to adsorb

(22) Hugel, T.; Grosholz, M.; Clausen-Schaumann, H.; Pfau, A.; Gaub, H.; Seitz, M. *Macromolecules* **2001**, *34*, 1039−1047.
(23) Friedsam, C.; Becares, A. D.; Jonas, U.; Seitz, M.; Gaub, H. E. *New J. Phys.* **2004**, *6*, 9.
(24) Cui, S. X.; Liu, C. J.; Wang, Z. Q.; Zhang, X. *Macromolecules* **2004**, *37*, 946−953.
(25) Chatellier, X.; Senden, T. J.; Joanny, J. F.; di Meglio, J. M. *Europhys. Lett.* **1998**, *41*, 303−308.
(26) Kühner, F.; Erdmann, M.; Sonnenberg, L.; Serr, A.; Morfill, J.; Gaub, H. E. *Langmuir* **2006**, *22*, 11180−11186.
(27) Hugel, T.; Seitz, M. *Macromol. Rapid Commun.* **2001**, *22*, 989−1016.
(28) Sonnenberg, L.; Parvole, J.; Kühner, F.; Billon, L.; Gaub, H. E. *Langmuir* **2007**, *23*, 6660−6666.
(29) Sonnenberg, L.; Parvole, J.; Borisov, O.; Billon, L.; Gaub, H. E.; Seitz, M. *Macromolecules* **2006**, *39*, 281−288.

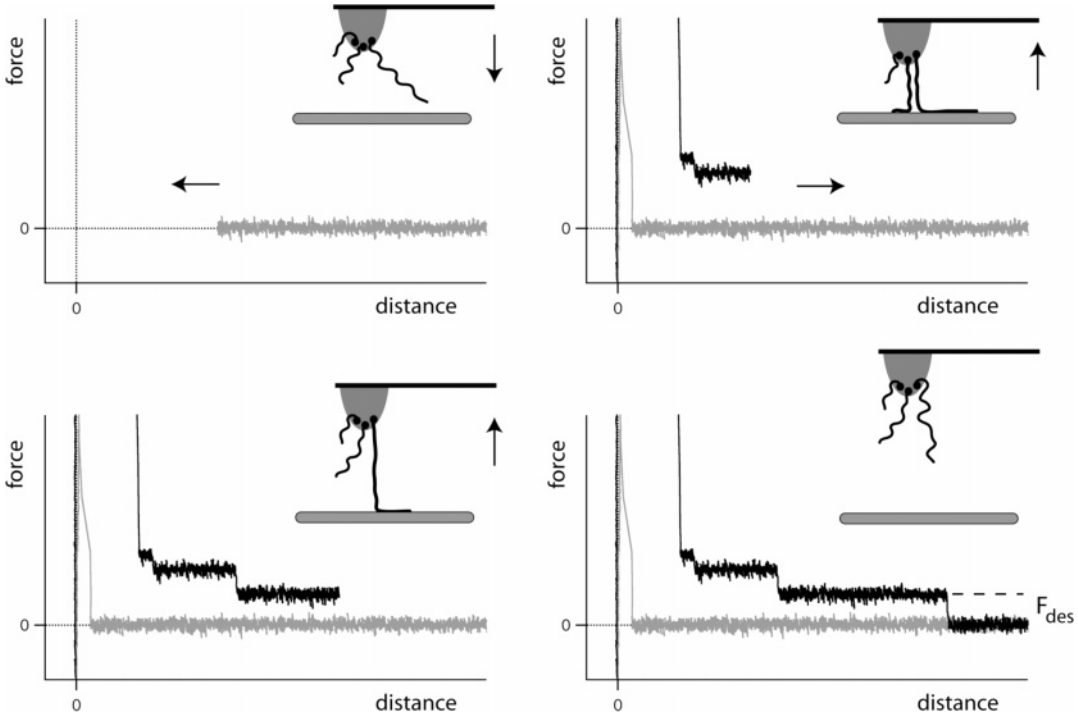

Figure 3. Illustration of a typical single molecule desorption experiment with polymer chains covalently attached to the tip of an AFM cantilever.

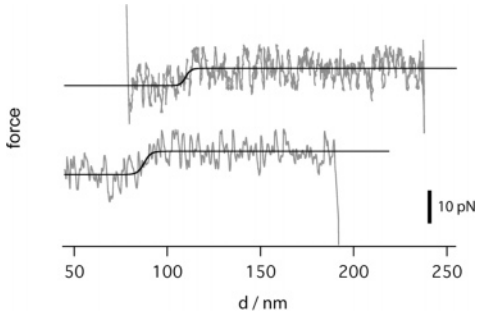

Figure 4. Two force versus distance curves of PEO-*b*-PLE obtained upon successive desorption from the calcite (104) surface. At a distance of about 100 nm the transition from desorbing ethylene oxide monomers to glutamate monomers can be seen. If the transition occurs at distances smaller than 100 nm, this is most probably because of the attachment point of the polymer at the curved AFM tip. The force regime is about 60 pN, the difference in force about 5 pN.

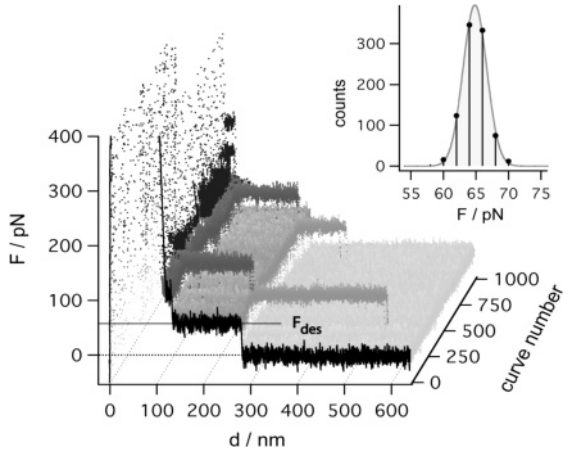

Figure 5. Measurement series consisting of 1000 force−distance curves (10 mM $CaCl_2$, pH 6). Note that only plateaus originating from desorption of PLE can be seen here because the unspecific adsorption peak at small distances hides desorption of PEO. In all curves the same molecule is probed. In addition from time to time a second molecule participates. The mean interaction force is obtained via statistical analysis of the plateau forces (see inset). A typical value for fwhm of the force histograms is 6 pN.

strongly onto a calcite crystal.[30] This is reflected by a sharp transition in force at a distance that coincides with the contour length of the PEO_{273} block (∼100 nm). Note that in Figure 4 the desorption of a single PEO-*b*-PLE polymer can be seen, whereas the staircase-like pattern in Figure 3 arises from the desorption of several polymer chains. In the curve presented in Figure 3 the force transition between the two blocks as shown in Figure 4 is not visible, as it is generally only rarely observed. This is first of all because PEO often does not adsorb on the calcite surface as was shown in desorption experiments with polyamine-*b*-PEO_{273} on calcite (data not shown). However, if a desorption plateau was observed, the desorption force equals the values as found for the PEO in the block copolymer. The finding of rare desorption events but still with "high" desorption force has already been reported in the literature previously for the adsorption of poly(acrylic acid) on self-assembled monolayers.[23] In addition to the reduced PEO adsorption, the "unspecific" peak at small distances in the force−extension curves often extends to the distance regime where the force transition is expected and therefore covers the force transition. This is in particular true when several polymers are adsorbed to the surface and/or the transition distance is shifted to shorter lengths because of the attachment point of the polymer on the curved AFM tip. Moreover, as soon as several polymers are desorbed in parallel, intramolecular interactions also contribute, smearing out the force transition such that it is not detectable anymore.

The strength of single molecule desorption measurements, namely the measurement of interaction forces with high precision and the possibility to resolve minute force differences, is illustrated in Figure 5. Therein a series of force−distance curves is shown, in which the same PEO-*b*-PLE molecule was probed over a thousand times. Calcite (104) was used as the solid surface. In the case of occasional contribution of a second chain, two plateaus can be seen in the spectra. The force transition between the two blocks is not observed here, as the unspecific adsorption peak at small distances exceeds the transition regime.

(30) Cölfen, H.; Qi, L. M. *Chem.-Eur. J.* **2001**, *7*, 106−116.

The mean desorption force of the glutamic acid with the calcite crystal is obtained by a statistical analysis of the plateau force of all curves that exhibit plateaus longer than 200 nm. In this case the PEO block with its contour length of 100 nm is not able to alter the interaction of the PLE with the calcite surface. The resulting force histogram is shown in the inset of Figure 5. A typical value for the full width at half-maximum (fwhm) is 6 pN; thus, the quantification of the mean desorption forces is possible with a precision of 1−2 pN.

Calcite Crystals. Calcite (104) was provided by R. U. Barz (Institut für Mineralogie, LMU München) as well as crystallized by Y. Luo (MPI-KG). In the desorption measurements no differences in the desorption forces were found for the different samples. Calcite (100) was purchased from MTI Corporation (Richmond, VA).

The Calcite (104) surface and (100) surface both consist of alternating Ca atoms and CO_3 groups. Differences between the two crystal faces exist in the distance of neighboring Ca−CO_3 and the orientation of CO_3 groups (see Supporting Information, Figures SI-5 and SI-6). However, calcite surfaces are not atomically flat in solution and can reform in solution by etch pits or dissolution-recrystallization. Even stable (104) cleavage planes reconstruct in moist air through pit formation and film growth.[31]

Control Measurements with Poly(L-glutamic acid). Poly(L-glutamic acid) was obtained from Sigma-Aldrich as sodium salt with a molar mass of 750−5000 g/mol (CAS Number 26247-79-0). Because of the broad molar mass distribution, mass/volume was chosen as the polymer concentration unit instead of molar concentration to have a constant number of monomer units independent of the polymer molar mass. A 1 mg/mL polymer solution was titrated with 10 mM $CaCl_2$ solution (see Supporting Information, Figure SI-3). ζ-potentials were determined with a Zetasizer (Malvern Instruments). Added $CaCl_2$ concentrations were chosen for a Ca^{2+} saturated polyanion solution on the basis of the $CaCl_2$ titration results (see Supporting Information, Figure SI-4).

Results and Discussion

pH-Dependent Interaction Forces between PLE and Calcite (104). The crystallization process in the presence of polymeric additives is strongly dependent on the experimental conditions such as pH or ionic strength of the solution. This was empirically demonstrated for $BaSO_4$ which has the advantage of a single polymorph with constant morphology over a wide range of pH and experimental conditions. However, the crystal morphologies could be varied to a large extent by different polymer additives[32] and different pH conditions, especially for polycarboxylates.[33] A general correlation between pH-variation and crystal morphology has not been established so far.

Desorption measurements were conducted in aqueous 10 mM $CaCl_2$ solution at varying pH between 6 and 12, and the mean desorption forces between PLE and calcite (104) were analyzed (see Figure 6). Thereby, the same mean desorption force of ca. 64 pN was obtained for pH 6 and pH 11 and a slight increase of ca. 4 pN was visible around pH 8.6.

This maximum position of the desorption force in Figure 6 corresponds to the literature-documented point of zero charge (pzc), which was reported to be between pH 8.2 and 9.5.[34,35] Therefore, at pH > 10 the calcite surface and the PLE are expected to be negatively charged, resulting in a repulsive

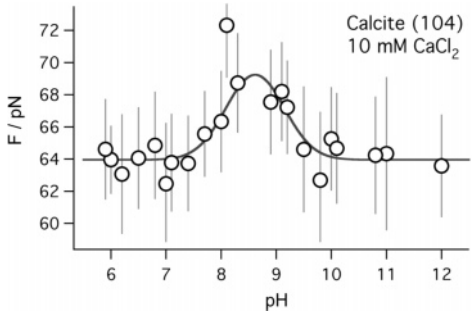

Figure 6. Mean desorption forces in dependence of the pH of the aqueous $CaCl_2$ solution. Each circle represents an independent measurement series as shown in Figure 3. Error bars represent the fwhm of the force histograms. An increased force is observed only between pH 8 and 9. In that regime, the calcite point of zero charge (pzc) is expected.

electrostatic contribution to the desorption force. As the pK_a of the PLE is <6,[36] an electrostatic attraction between the positively charged calcite surface[37−40] and the negatively charged polymer should be expected at pH 6−8, resulting in the highest desorption force in absence of Ca^{2+}. However, this is clearly not observed in Figure 6, as our experiments were conducted in an excess of 10 mM Ca^{2+}, and more importantly, the desorption force stays constant below pH 7 and above pH 10.

On the basis of the interaction forces between PLE and calcite (104) in dependence of the salt concentration of the aqueous solution (see further below, Figure 7), some additional comments can be given on the pH-dependent interaction forces. First, when screening all electrostatic interactions between polymer and calcite surface at high salt concentrations, the desorption force equals the desorption force found at pH 8−9. One can therefore conclude that no electrostatic interactions are contributing to the overall desorption force in this regime. Second, when decreasing the salt concentration (increasing electrostatic interactions) at pH 6, the desorption force decreases. That is, the electrostatic interaction between polymer and surface is repulsive. From the shape of the curve in Figure 6, one would then conclude that the electrostatic interaction at pH > 9 is repulsive, too. However, note that because of the small force differences obtained as a function of the pH, electrostatic interactions are supposed to be weak. This corresponds either to a weakly charged polymer, a weakly charged surface, or both.

It is known that complexation of Ca^{2+} and polymers bearing carboxylic groups can occur as a function of the accessible carboxylate functions[41,42] introducing positive charges into the side chains. We have therefore looked at the Ca^{2+} binding of PLE at the relevant pH values by titration experiments and found the expected higher Ca^{2+} binding at higher pH as compared to the lower pH (see Supporting Information). Electrokinetic measurements further showed that the ζ-potential of poly(L-glutamic acid) saturated with Ca^{2+} in solution is still negative (−10 mV at pH 6 and −35 mV at pH 11) but considerably less negative than that of the polymer itself (−65 mV) (see

(31) Kendall, T. A.; Martin, S. T. *J. Phys. Chem. A* **2007**, *111*, 505−514.
(32) Qi, L. M.; Cölfen, H.; Antonietti, M. *Angew. Chem., Int. Ed.* **2000**, *39*, 604−607.
(33) Qi, L. M.; Cölfen, H.; Antonietti, M. *Chem. Mater.* **2000**, *12*, 2392−2403.
(34) Moulin, P.; Roques, H. *J. Colloid Interface Sci.* **2003**, *261*, 115−126.
(35) Churchill, H.; Teng, H.; Hazen, R. M. *Am. Mineral.* **2004**, *89*, 1048−1055.
(36) Schlaad, H. *Adv. Polym. Sci.* **2006**, *202*, 53−73.
(37) Vancappellen, P.; Charlet, L.; Stumm, W.; Wersin, P. *Geochim. Cosmochim. Acta* **1993**, *57*, 3505−3518.
(38) Fenter, P.; Geissbuhler, P.; DiMasi, E.; Srajer, G.; Sorensen, L. B.; Sturchio, N. C. *Geochim. Cosmochim. Acta* **2000**, *64*, 1221−1228.
(39) Pokrovsky, O. S.; Mielczarski, J. A.; Barres, O.; Schott, J. *Langmuir* **2000**, *16*, 2677−2688.
(40) Lin, Y. P.; Singer, P. C. *Geochim. Cosmochim. Acta* **2005**, *69*, 4495−4504.
(41) Madsen, F.; Peppas, N. A. *Biomaterials* **1999**, *20*, 1701−1708.
(42) Kriwet, B.; Kissel, T. *Int. J. Pharm.* **1996**, *127*, 135−145.

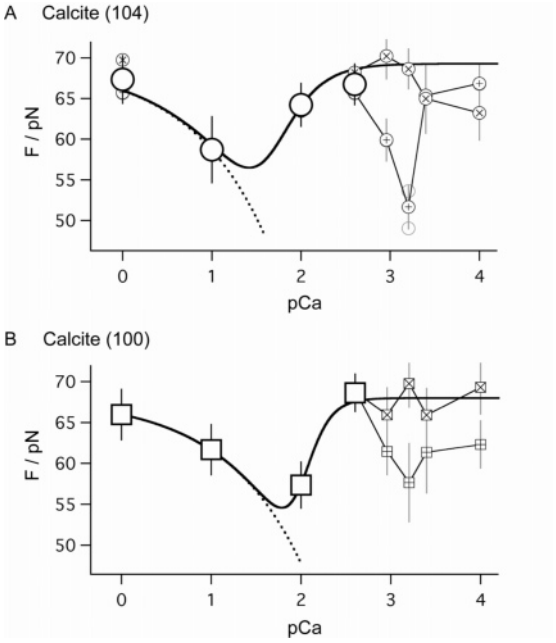

Figure 7. Mean desorption forces in dependence of Ca-concentration in solution (pCa = −log[Ca]) for A) calcite (104) and B) calcite (100) at pH 6. Two independent measurement series as shown in Figure 3 were performed at every pCa value (small symbols). In the regime pCa < 2.5 the measured desorption forces are highly reproducible; large symbols represent weighted averages of the two data points. Data points were fit by $F = F_0 + \alpha\sigma\tau[\mathrm{Ca}]^{-0.5}$ with α = const., the surface potential σ = const. and the polymer charge density τ. For $\tau = 1$ (dotted curve) the fit function shows the dependence of the desorption force on electrostatic screening (Debye screening length $\kappa^{-1} \propto [\mathrm{Ca}]^{-0.5}$); a variable charge density due to, for example, charge regulation mechanisms was modeled with a titration behavior, $\tau = 1/(1 + \exp[(\mathrm{pCa} - \mathrm{pD})/t])$ (solid line).

Supporting Information). This is because the partial neutralization of the polymer is due to the Ca^{2+} coordination. Nevertheless, a further shift of the ζ-potential occurs upon addition of a large excess of Ca^{2+}, from −35 mV to −20 mV at pH 11 (see Figure SI-4).

The Ca^{2+} coordination to the carbonate groups can be expected in a manner similar to that for the polymer carboxyl groups, which leads to the repulsion of a polymer with pH-dependent negative charge from an almost neutral crystal surface. This could be an explanation for the repulsive components yielding the reduced desorption force observed at pH > 10.

At the pzc, one expects an equal distribution of calcium and carbonate ions at the surface. When decreasing the pH from pH > 10 to pzc, the calcite surface becomes more and more uncharged and with it the electrostatic repulsion between PLE and calcite less and less pronounced. As a consequence, the measured desorption forces rise in that pH regime. For pH < pzc, the electrostatic interaction between PLE and calcite is repulsive again, such that the maximum of the desorption force in Figure 6 reflects the pzc of the calcite surface.

The observed results for the desorption force at pH < 8, namely a weak electrostatic repulsion between PLE and calcite, were the most unexpected findings of the pH-dependent measurements. At this pH (pH < pzc), the calcite surface has to be expected as Ca^{2+} terminated, but the polymer will still be neutral to slightly negatively charged (see above). In other words, even in the presence of Ca^{2+} in solution a marginally higher desorption force than that at pH = pzc would be expected. However, this conclusion is drawn from a separate consideration of the properties of the polymer and calcite surface but not as a whole. In agreement to our findings for pH < 8, namely that the polymer interacts with a seemingly negatively charged calcite surface at pH < pzc, Seitz et al. found an attractive/repulsive electrostatic interaction between poly(vinyl amine)/poly(acrylic acid) and calcite in NaCl solution at pH 6. This also corresponded to a seemingly negatively charged calcite surface.[17]

When comparing desorption measurement series in dependence of the pH, qualitative differences in adsorption behavior were observed. At pH > 10 the probability of observing desorption events in the force−extension spectra is decreased (e.g., the consecutive observation of 1000 desorption plateaus as shown in Figure 3 is extremely unlikely), which is also reflected in the smaller number of data points in this pH regime in Figure 6. That is, for PLE molecules adsorption on the calcite surface is less favorable at pH > 10 than at pH < 8. These different adsorption characteristics may also be regarded as a hint that the mechanisms that result in the repulsion between PLE and calcite are different for the two pH regimes. For pH > 10, PLE and calcite are similarly charged and therefore experience "real" electrostatic repulsion, which may act as an adsorption barrier. For pH < 8, PLE and calcite are expected to be oppositely charged so that adsorption may be advantageous. In this case one would have to conclude that the measured electrostatic repulsive force is induced by the adsorption of the PLE on the calcite surface. ζ-Potentials indicate further Ca^{2+} coordination by the polymer at Ca^{2+} excess, which would be expected near the calcite surface under the conditions at pH < pzc.

In general, the properties of surface-adsorbed polyelectrolytes can be significantly changed with respect to the same molecules in solution, e.g., the dissociation equilibrium can vary upon adsorption.[43−45] Such effects may be even more pronounced at dielectric boundaries because of image charge interactions, which are for example opposing at low dielectric surfaces.[46,47] In particular, charge reversal has been predicted for semiflexible polyelectrolytes on charged planar surfaces.[48,49]

Our findings reveal that the simple epitaxial or even electrostatic view on polymer−crystal interactions is too simplified to explain the experimental findings and that quantitative AFM force spectroscopy can yield atomic details of the additive interaction with a crystal surface in a quantitative manner. Moreover, they point out the ability of this technique to monitor even small differences in molecular properties arising from the adsorption of polyelectrolyte molecules on charged surfaces. However, further experiments will be needed to elucidate the detailed individual contributions of the polymer upon interaction with a crystal surface.

pCa-Dependent Interaction Forces between PLE and Calcite (104)/Calcite (100). Concluded from the above results, the synthesis of biomimetic materials on the basis of calcium carbonates may further be crucially dependent on the calcium

(43) Burke, S. E.; Barrett, C. J. *Langmuir* **2003**, *19*, 3297−3303.
(44) Sukhishvili, S. A.; Granick, S. *Langmuir* **2003**, *19*, 1980−1983.
(45) Xie, A. F.; Granick, S. *Nat. Mater.* **2002**, *1*, 129−133.
(46) Netz, R. R. *J. Phys.: Condens. Matter* **2003**, *15*, S239−S244.
(47) Netz, R. R. *Phys. Rev. E* **1999**, *60*, 3174−3182.
(48) Netz, R. R.; Joanny, J. F. *Macromolecules* **1999**, *32*, 9013−9025.
(49) Boroudjerdi, H.; Kim, Y. W.; Naji, A.; Netz, R. R.; Schlagberger, X.; Serr, A. *Phys. Rep.* **2005**, *416*, 129−199.

concentration. Among the polymer−crystal interactions, electrostatic ones should be most affected by a variation of the ionic strength of the solution. The importance of electrostatic interactions was recently pointed out by Volkmer et al., who found that the charge density of an organic template layer is of importance for tuning the $CaCO_3$ crystallization process with respect to polymorph selection and crystal orientation under monolayers.[50]

Desorption experiments were performed at pH 6 of an aqueous solution containing between 0.1 mM and 1 M $CaCl_2$. The corresponding mean desorption forces plotted versus pCa $= -\log[Ca]$, with [Ca] being the concentration of Ca^{2+} ions in solution, are shown in Figure 7 for two very similar calcite faces: (104) and (100). For both surfaces a similar behavior and force differences smaller than 10 pN were observed. It was found that the desorption forces are highly reproducible at salt concentrations $0 < \text{pCa} < 2.5$ and nonreproducible at pCa > 2.5 (see Figure 7).

For interpretation of the findings, two salt-dependent contributions to the desorption force have to be considered: electrostatic screening and polymer charge density.[17] In Debye−Hückel approximation the electrostatic contribution to the desorption force is proportional to the surface potential σ, the Debye screening length κ^{-1} ($\propto [Ca]^{-0.5}$) and the linear (polymer) charge density τ: $F_{el} \propto \sigma\kappa^{-1}\tau$. The desorption force then consists of a non-Coulomb contribution F_0 and the electrostatic desorption force F_{el}. The experimental data were therefore fit by the following formula: $F_{des} = F_0 + \alpha\sigma\tau[Ca]^{-0.5}$ with α being a constant and [Ca] the fit variable. The surface potential σ was also regarded as constant.

At high salt concentrations the polymer is maximally charged ($\tau = 1$) and the desorption force is a function of the ionic strength of the solution. However, $\tau = 1$ does not correspond to a fully charged PLE polymer under the given experimental conditions because of Ca^{2+} complexation (see above). At pCa $= 0$ electrostatic interactions between polymer and surface are almost completely screened, i.e., $F_{des} \approx F_0$. When decreasing the calcium concentration to pCa $= 1$, the PLE is still charged ($\tau = 1$) but electrostatic interactions with the calcite are less screened and not negligible any more, i.e., $F_{el} \neq 0$. In this regime of "high" ionic strengths, the desorption force decreases proportional to the Debye screening length (dotted lines in Figure 7). This means that a repulsive interaction, $F_{el} < 0$, between PLE and calcite surface has to be assumed at pH 6! It may be interesting to note that the ratio of the fitted surface potentials $\sigma_{104}/\sigma_{100} = 1.7$ is of the same order of magnitude as the ratio of the density of surface ions (number of ions divided by the surface area; see also Supporting Information), $\rho_{104}/\rho_{100} = 2.1$. This may be interpreted as a hint that the differences in the measured desorption force between the two crystal surfaces are caused by different electrostatic interactions.

With decreasing salt concentrations, a phenomenon known as charge regulation has to be taken into account.[49,51] The charge density of all objects with dissociable groups, as for example weak polyelectrolytes, is a function of the salt concentration because of repulsive charge interactions within the polymer. These intramolecular repulsions counter the dissociation reaction of the carboxylic groups of the poly(L-glutamic acid). As electrostatic interactions are stronger at low salt concentrations (less screening), charge regulation is more pronounced, too. Thus, the polymer charge density decreases with decreasing salt concentration. Using the same argument, the charge density of a surface adsorbed polymer is furthermore altered by the surface charges and vice versa.

In order to fit the experimental data the polymer charge density was modeled with a titration behavior in dependence of pCa ($\tau = 1/(1 + \exp[(\text{pCa} - \text{pD})/t])$, solid lines in Figure 7). Deflection points of the titration functions were found to be at $\text{pD}_{104} = 1.6$ for the calcite (104) and at $\text{pD}_{100} = 2.0$ for the calcite (100) surface. This finding is in qualitative agreement with the surface charge densities of the calcite surfaces. The larger charge density of the calcite (104) surface in comparison to the calcite (100) surface leads to a reduction of the polymer charge already at higher salt concentrations, i.e., lower pCa values.

The desorption forces in the nonreproducible regime at low salt concentrations (pCa $\approx$ 3) are dependent on the AFM tip, i.e., the set of molecules. This may again be correlated with the complexation of Ca^{2+} ions by the PLE polymer. Because of the attachment process of the triblock polymer to the AFM tip, the number of bound polymer chains can only be roughly controlled and is not known, as generally much more polymers are bound to the tip than seen in the experiments (e.g., because of the tip's curvature). Thus, the degree of Ca^{2+} complexation at low salt concentrations, when the number of carboxylic groups in the PLE polymers is comparable to the number of available Ca^{2+} ions in solution, may depend on the AFM tip used. However, the effect may also be caused by the calcite surface itself, as in electrophoretic mobility studies a variation of the ζ-potential of calcite (104) was observed at a similar salt concentration.[34]

The results on the two calcite faces (104) and (100) shown in Figure 7 indicate that the desorption forces are delicately dependent on electrostatic interactions. It is a remarkable observation that significant differences of the desorption forces could be detected for the structurally similar calcite faces (see, e.g., pCa = 2 in Figure 7).

Conclusions

In polymer-controlled crystallization processes, small variations on the molecular level can result in large morphological effects on the macroscopic level. We quantitatively investigated the molecular forces between poly(L-glutamic acid) and calcite on the single molecule level and showed that a variation of pH and calcium concentration of the solution as well as a variation of the crystal face led to variations of the interaction forces of comparable strength. The observations underscore that a complex interplay of molecular interactions has to be assumed for polypeptide−mineral systems. We demonstrated that quantitative AFM-based desorption measurements are able to enlighten this interplay on the basis of the molecular interaction forces with very high precision although the nature of the detected interactions is not yet clear in all cases. In particular, this approach should also be able to give insight into the dynamics of crystal growth in the presence of polymers, as it involves not only the adsorption but also the (transient) desorption and conformational rearrangements of polymer chains at the mineral

(50) Volkmer, D.; Fricke, M.; Agena, C.; Mattay, J. *J. Mater. Chem.* **2004**, *14*, 2249−2259.
(51) Friedsam, C.; Gaub, H. E.; Netz, R. R. *Europhys. Lett.* **2005**, *72*, 844−850.

surface. This could help to correlate molecular interactions and conformations with macroscopic crystal properties and thus to control the crystallization and materials properties.

Acknowledgment. Helpful discussions with Dr. Paul Bowen (EPFL, Lausanne), Prof. Lennart Bergström (University of Stockholm), Prof. Thomas Vilgis (MPI Mainz), and Prof. Roland Netz (TU München) are gratefully acknowledged. We thank Margit Barth (MPI-KG) for the assistance with the $CaCl_2$ titrations of poly(L-glutamic acid) and Heidi Zastrow (MPI-KG) for ζ-potential measurements. This work was supported by the Deutsche Forschungsgemeinschaft (grants CO 194/1-1, SE 888/3-1, and SFB 486) and the Fonds der chemischen Industrie.

Supporting Information Available: Polymer synthesis (^{1}H NMR, SEC), titration of poly(L-glutamic acid) with $CaCl_2$ at different pH, ζ-potential measurements of poly(L-glutamic acid), and illustrations of calcite (104) and (100) surfaces. This material is available free of charge via the Internet at http://pubs.acs.org.

JA074070I